Sensors and Actuators B 228 (2016) 43–52

Contents lists available at ScienceDirect

Sensors and Actuators B: Chemical

journal homepage: www.elsevier.com/locate/snb

Impedimetric non-enzymatic glucose sensor based on nickel hydroxide thin film onto gold electrode

Ana L. Rinaldi, Romina Carballo*,[1]

IQUIFIB, National Research Council (CONICET), Faculty of Pharmacy and Biochemistry, University of Buenos Aires, Junin 956, CP 1113 Buenos Aires, Argentina

ARTICLE INFO

Article history:
Received 17 September 2015
Received in revised form
24 December 2015
Accepted 29 December 2015
Available online 4 January 2016

Keywords:
Glucose
Non-enzymatic sensor
Nickel gold electrode
Electrochemical impedance spectroscopy
Blood sample

ABSTRACT

A non-enzymatic glucose sensor based on a thin layer of nickel immobilized on a gold electrode ($EAuNi(OH)_2$) was used to perform impedimetric determination of glucose. The electrodeposition solution, composed of 0.010 M $Ni(NO_3)_2{\cdot}6H_2O$ and 1 M of chloride, allows only one active catalyst (NiOOH) to be present on the gold electrode surface after activation with 0.1 M KOH.

Electrochemical oxidation of glucose on $EAuNi(OH)_2$ electrode was evaluated by Cyclic Voltammetry (CV) and Electrochemical Impedance Spectroscopy (EIS) in the concentration range of 0–14.8 mM of analyte. $Ip/v^{1/2}$ vs scan rate graph shows a typical catalytic behavior by $EAuNi(OH)_2$ toward glucose oxidation. Measurements in the presence of possible interfering species (ascorbic acid, uric acid, dopamine) did not affect the response of the analyte of interest.

EIS offers good sensibility and selectivity for the glucose detection by non-enzymatic glucose sensor as an alternative to conventional methods. A single-frequency impedance method is proposed as transduction principle. For that, the parameters of complex impedance (module, phase, real and imaginary impedance) at each frequency were evaluated in function of glucose concentration and in terms of correlation coefficient. These analyses show a better linear response for the module of impedance (|Z|) in the range of 0–2 mM of glucose at 0.1 Hz ($R^2 = 0.984$) with a slope of 484.7 $\Omega\,mM^{-1}$ of glucose. Finally, $EAuNi(OH)_2$ was successfully applied to the assay of glucose in blood samples.

1. Introduction

Demand for monitoring glucose in the food industry, biotechnology and clinical diagnosis has been growing in recent years, accompanied by a steady increase in the number of proposed devices. Basically, glucose electrochemical sensors can be divided into two categories: enzymatic and non-enzymatic electrochemical sensors [1]. In some way, many investigations have been undertaken on non-enzymatic glucose sensors (NEG) in order to overcome the disadvantages of enzymes and mediators in biosensors [2,3]. NEG sensors constitute the fourth generation of glucose sensor technology, which are easier to prepare, cheaper, and have higher stability compared with traditional glucose sensors [4].

Unlike biosensors where the enzyme acts as a catalyst, in NEG sensors the nature of the modifier is of great importance since atoms at the surface of the electrode act as the electrocatalysts [5]. Although in some cases the mechanism of glucose oxidation at the electrode surface is still not fully understood, a variety of materials including the noble metals [6–8], metal oxides/hydroxides [9,10], carbon nanotubes [11], graphene [12], polymers, and hybrids [13,14] have been explored as NEG sensors in their response to the electrocatalytic oxidation of glucose. In an effort to expand on synergically catalytic effects of different metal oxides, metal oxide/metal oxide (bimetallic oxide) composites have been proposed for NEG sensors [15,16]. In other cases, metal/metal oxide combinations have been explored in order to integrate advantages of both metals (support) and metal oxides (modifier). In the latter device, two aspects can significantly affect the electrochemical performance of the sensor: (1) the properties of the support electrode, such as large specific surface area, its geometry, and high electron transfer rate, and (2) the method of preparation of the metal oxide and its interaction with the support electrode [17–20].

In particular, $Ni(OH)_2$-based non-enzymatic glucose sensors have excellent electrocatalytic activity toward glucose oxidation, which is mediated by $Ni^{(II)}/Ni^{(III)}$ redox couples in alkaline medium [21]. The electrochemical preparation of particles, nanoparticles,

* Corresponding author.
E-mail addresses: rocar@ffyb.uba.ar, romina.carballo191278@gmail.com (R. Carballo).
[1] CONICET permanent staff.

http://dx.doi.org/10.1016/j.snb.2015.12.101
0925-4005/

and films of nickel from a solution containing this metal ion has been investigated intensely during the last decades, even onto the bare support electrode [22,23]. Many adjustable parameters, such as the deposition potential or current, time, temperature, pH, and electrolyte composition, allow to adjust the size, shape, thickness, and spatial distribution of the electrodeposited nickel. Moreover, numerous devices have been prepared by cathodic electrodeposition of nickel on both traditional and nanostructured electrode surfaces such as boron doped diamond [24,25], carbon [26,27] or graphite [28,29]. However, as previously mentioned, it is interesting to note that the interaction between the support material and the metal oxide can be used to modify the electrocatalytic activity of the latter or even enhance it greatly, such as in the case of gold electrodes for electrochemical evolution of oxygen [30]. In NEG sensors, mixed Au/Ni surface oxide electrodes have been studied, in which the electrooxidation of glucose is due to the presence of two catalysts such as Au(OH) ads and NiOOH without any synergistic interaction between them [31–35].

Amperometry is probably the most popular electrochemical technique applied in the glucose sensors. Nonetheless, in the last years the use of electrochemical impedance spectroscopy (EIS) has been proposed as a transduction principle in these sensors. In this new technology, electrochemical impedance spectroscopy is more useful to study the analyte in lower concentrations, the electrode/electrolyte interface and the electrode surface kinetics. It also provides the advantages of cheap measurement, no sample pretreatment and the possibility to detect any kind of molecule, when an interaction between recognition surface and analyte occurs. The advantage of EIS over DC techniques is that this steady-state technique is capable of probing relaxation phenomena over a wide frequency range, making high precision measurements since the response may be indefinitely steady and can therefore be averaged over a long period of time. Both types of Faradaic EIS, with and without redox probe introduction, are based on the evaluation of the change of charge transfer resistance (R_{ct}) as a function of glucose concentration [36,37]. In all cases, R_{ct} must be obtained from an elemental electrical circuit fitted to a set of impedance values, which have been measured over a frequency range. This makes the use of EIS become tedious and sometimes excessively long. As an alternative, a single-frequency analysis could be applied. In this case, the fitting procedure is not necessary, although optimal parameters of complex impedance, frequency and voltage values of the system must be previously determined. However, very few reports have employed this methodology and, those which have applied it, are mostly glucose biosensors [38,39].

In this work, a gold electrode substrate modified by electrochemical deposition of thin films of nickel hydroxide, designated as EAuNi(OH)$_2$, is characterized and employed as non-enzymatic glucose sensor based on the EIS. The properties of both Ni(OH)$_2$/NiOOH and the material of the electrode are discussed. The experimental conditions of the impedance measurements that enable the determination of glucose in blood at a single frequency were also optimized.

2. Experimental

2.1. Materials

All chemicals used in this work were of analytical grade and were purchased from Merck and Sigma–Aldrich, and they were used as received, without further purification. Deionized water was used for all aqueous solutions.

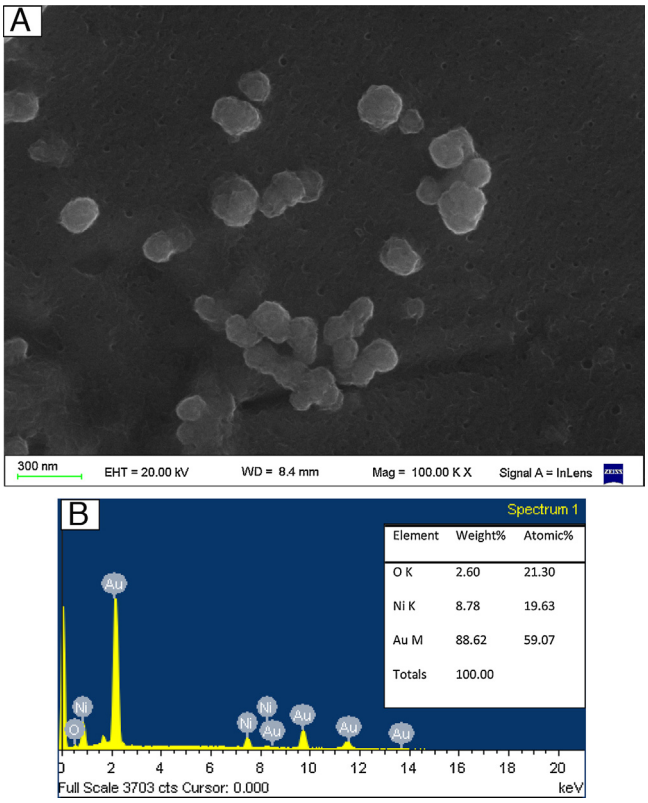

Fig. 1. (A) SEM image of EAuNi(OH)$_2$ (magnification 100000×). (B) Energy dispersive X-ray analysis exploring the elemental composition of metals in EAuNi(OH)$_2$ electrode.

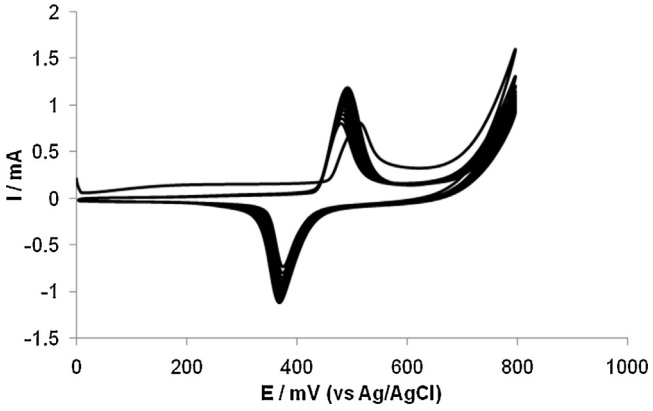

Fig. 2. Cyclic voltammograms corresponding to the activation of EAuNi(OH)$_2$ in 0.1 M KOH solution. Scan rate 50 mV s^{-1}, 15 cycles.

2.2. Apparatus

Cyclic voltammetries (CVs) and amperometric measurements were performed with a purpose built potentiostat (TEQ-Argentina), with digital signal generator for implementation of different electrochemical techniques. Electrochemical impedance spectra were recorded using a potentiostat TEQ4-Z (TEQ-Argentina) and a frequency response analyzer. Data analysis was performed with the program ZView® (Scribner Associates, USA). A gold working electrode (0.36 cm^2 geometric surface area), a Ag/AgCl KCl 3 M reference electrode (BAS) and a platinum wire auxiliary electrode were used for voltammetric and electrochemical impedance experiments. A purpose built Teflon cell was used in impedance measurements.

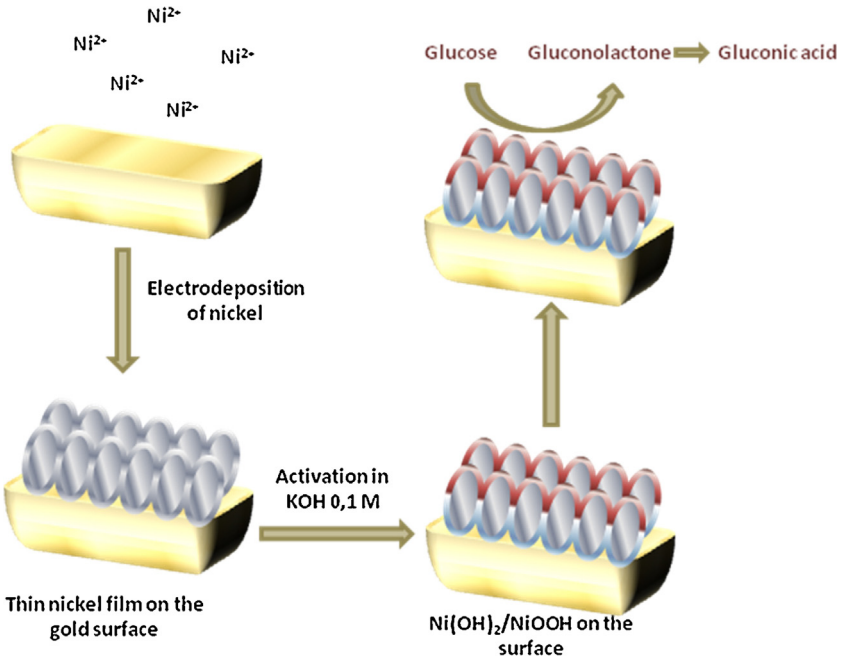

Scheme 1. Schematic representation of the gold electrode modification process.

Scanning electron microscopy (Zeiss DSM982 GEMINI SEM with Field Emission Gun) and energy dispersive X-ray spectroscopy (EDS INCA ENERGY, Oxford Instruments) were used to characterize the morphology and structure of the $EAuNi(OH)_2$.

2.3. Preparation of the modified electrodes

Gold electrodes used for electrochemical experiments were thoroughly cleaned by immersions in "Piranha" solution (H_2SO_4:H_2O_2/3:1) for 24 h, then rinsed with MilliQ water and dried with nitrogen stream.

A non-deaerated solution of 0.010 M $Ni(NO_3)_2{\cdot}6H_2O$ and 1 M NH_4Cl at pH 5 was used for electrochemical deposition of nickel to obtain $EAuNi(OH)_2$ after the activation in alkaline medium. Firstly, the process involves electrochemical nucleation and growth of nickel particles from nickel solution onto the gold electrode [22]. Electrodeposition of nickel was carried out by applying a potential step of −1.3 V vs reference electrode for 60 s. Then, the film was activated by cycling between 0 and +0.80 V in aqueous 0.1 M KOH solution for at least 15 cycles at 50 mV s^{-1} until reproducible peak shape was obtained. The same procedure was applied at modified glassy carbon electrode ($GCNi(OH)_2$).

$EAu(OH)Ni(OH)_2$ was prepared following the procedure in [27] by potentiostatic deposition of nickel from a 0.10 M acetate buffer solution (pH 4.0) containing 0.001 M $Ni(NO_3)_2{\cdot}6H_2O$.

The nickel surface concentration (Γ_{Ni}), was estimated by integration of the cathodic wave at about 0.38 V corresponding to the $Ni^{(III)}/Ni^{(II)}$ reduction process obtained in 0.1 M KOH solution (50 mV s^{-1}) and referred to the 15th cycle, assuming that all the nickel redox sites are electroactive on the voltammetric time scale. The true surface area of the gold electrode, as determined by integration of Au oxide reduction peaks [40], was considered; this area was about 1–1.3 cm^2. For a set of ten $EAuNi(OH)_2$ modified electrodes, the average surface coverage of nickel was estimated in 4.9×10^{-9} mol cm^{-2}, with a relative standard deviation of 14%.

2.4. Electrochemical measurements

All electrochemical experiments were carried out in 0.1 M KOH and at room temperature.

The scan rate range in cyclic voltammetry (CV) was 0.001 V s^{-1} to 1 V s^{-1}.

Electrochemical Impedance Spectroscopy (EIS) was used to evaluate the performance of the sensor. This technique implies the application of an alternate current (AC) rather than a continuous one (DC). In order to obtain the optimal frequency, a frequency range of 100 kHz–0.1 Hz was used for impedance spectroscopic measurements. The amplitude of oscillation (AC) was set to 10 mV_{RMS}. The optimal working potential was set to +0.600 V and +0.500 V for measurements of glucose with and without blood sample, respectively. Module of impedance (|Z|) at 0.1 Hz was used to evaluate the response of the sensor.

CV measurements were performed in a glucose concentration range of 0–6.6 mM, while in the case of impedance, concentrations of 0–14.8 mM were evaluated.

Possible interfering species were tested at low concentrations (normal physiological levels [1]) of 0.08 mM for ascorbic acid, 0.4 mM for uric acid and 0.05 mM for dopamine. High concentrations of these analytes were also tested (0.3 mM for ascorbic acid, 2 mM for uric acid and 0.2 mM for dopamine).

2.5. Real sample analysis

To evaluate the applicability of the $EAu(NiOH)_2$ for analysis in real samples, the sensor was applied to the determination of glucose in blood samples.

For the impedance measurements, the working solutions were prepared so that the blood samples are spiked with glucose standard with respect to a lower glycemia. Here, 500 μL of blood sample (3.7 mM or 74 mg dL^{-1} of glucose measured by a commercial handheld glucose meter) and known concentrations of glucose standard (0, 0.1, 0.2, 0.3, 0.45, 0.58, 0.7, 0.8, 0.9, 1, 1.15, 1.3, 2 mM) were added to 5 mL of 0.1 M KOH.

Then, additional blood samples ($n = 3$) were also diluted ten times in 0.1 M KOH and were measured using the proposed

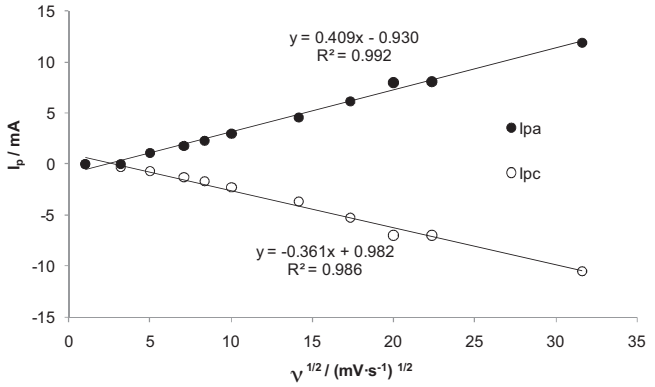

Fig. 3. Plots of the cyclic voltammetric (●) anodic and (○) cathodic peak currents against $\nu^{1/2}$ for EAuNi(OH)$_2$ in 0.1 M KOH solution.

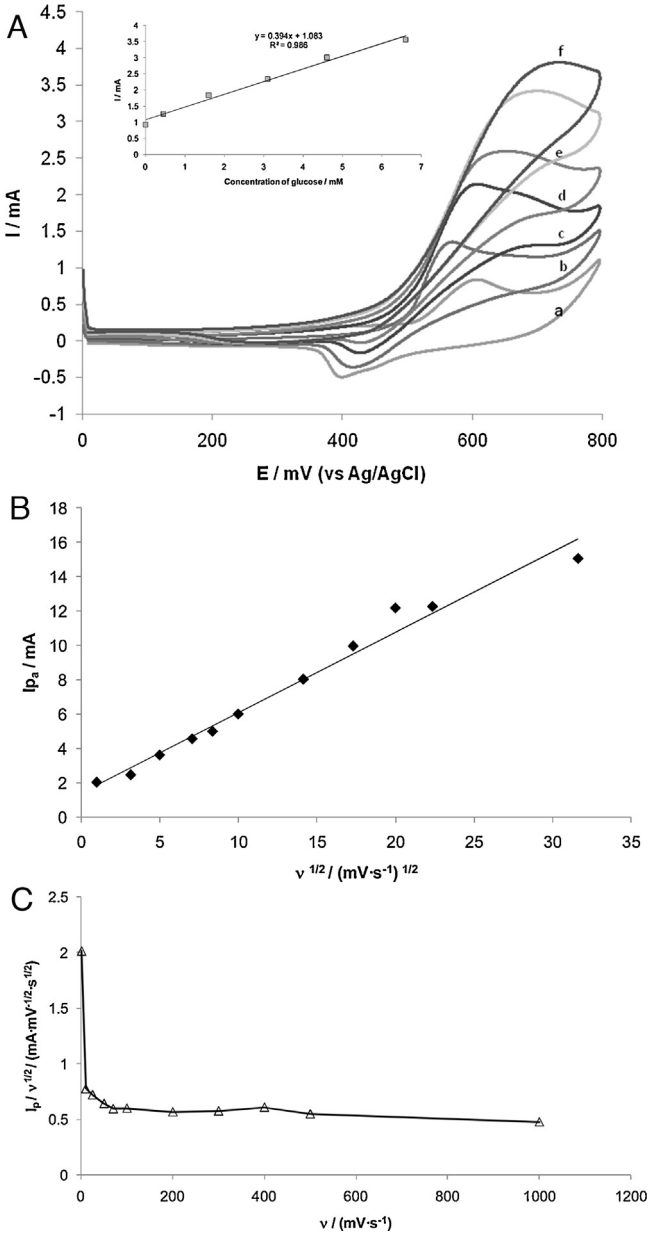

Fig. 4. (A) Cyclic voltammograms of EAuNi(OH)$_2$ in the presence of increasing concentrations of glucose: (a) 0, (b) 0.452, (c) 1.6, (d) 3.1, (e) 4.6, and (f) 6.6 mM. Inset: plot current vs glucose concentrations for EAuNi(OH)$_2$.(B) Plot of anodic peak current against $\nu^{1/2}$, for a concentration of glucose of 6.6 mM. (C) Plot of anodic current function ($I_p/\nu^{1/2}$) against the scan rate (ν), for a concentration of glucose of 6.6 mM.

methodology. The results were compared with those obtained by the commercial handheld glucose meter.

3. Results and discussion

3.1. Morphological and electrochemical characterization of the modified electrode

The nickel hydroxide thin film onto gold electrode (EAuNi(OH)$_2$) was prepared following a modified and optimized procedure proposed in the literature, as shown in Scheme 1. It briefly consisted of the cathodic electrodeposition of nickel and its subsequent activation in alkaline medium. In the first step, the gold electrode was placed in an acid solution of 1 M NH_4Cl containing 0.010 M nickel nitrate and was held at a negative potential (−1.3 V) in order to electrodeposit metallic nickel. Thus, at low $Ni(NO_3)_2$ concentrations, the Faradaic efficiency of the deposition of nickel is nearly 100% [41]. Moreover, the high chloride concentration could be modulating the deposition and electrocatalytic activity of $Ni^{(II)}/Ni^{(III)}$ onto the gold substrate thanks to the presence of chloride ions on this surface which enhance reduction and nucleation of nickel instead of evolution of protons [42]. It is possible to describe the mechanism of nickel deposition in which the resulting $NiCl^+$ species diffuses from bulk to gold electrode surface where it is adsorbed, as shown in the following equations (Eq. (1)) [43]:

$$Ni(NO_3)_2 \rightarrow Ni^{2+} + 2NO_3^-$$

$$NH_4Cl \rightarrow NH_4^+ + Cl^-$$

$$Ni^{2+} + Cl^- \leftrightarrow NiCl^+$$

$$NiCl^+ \leftrightarrow NiCl^+_{ads}$$

$$NiCl^+_{ads} + e^- \leftrightarrow NiCl_{ads}$$

$$NiCl_{ads} + e^- \leftrightarrow Ni + Cl^-$$

Next, the modified electrode was conditioned in 0.1 M KOH solution by potential cycling from 0.0 to +0.80 V at a sweep rate of 50 mV s^{-1} for about 15 cycles of potential scans for the electrochemical preparation of the active and stable $Ni(OH)_2$ (Eq. (2)):

$$Ni + 2OH^- \rightarrow Ni(OH)_2 + 2e^-$$

The morphology and elemental composition of the electrodeposited nickel structures on the gold electrode in alkaline medium are shown in the scanning electron microscopy (SEM) image and energy dispersive X-ray microanalysis (EDX) spectra of Fig. 1A and B, respectively. The size of nickel hydroxide nanoparticles measured from the SEM image was about 190 nm (Fig. 1A). The EDX analysis, employed for elemental identification, confirmed the presence of nickel and nickel hydroxide onto the gold surface (Fig. 1B).

Fig. 2 shows the evolution of the cyclic voltammograms for the enrichment of the $Ni(OH)_2$ species at the surface of the gold electrode. The enhanced baseline current of the first cycle is associated with the oxidation of Ni to $Ni^{(II)}$. Then, the anodic and cathodic peaks corresponding to $Ni^{(II)}/Ni^{(III)}$ redox couple are observed at about 0.48 and 0.38 V vs Ag/AgCl, at a scan rate of 50 mV s^{-1}, respectively. The peak currents increased gradually during successive scans until a steady state was reached. In alkaline solutions $Ni(OH)_2$ was oxidized to NiOOH and turned to $Ni(OH)_2$ by potential cycling [1].

The activity of Ni electrocatalysts is known to differ depending on the manner of electrode preparation. Therefore, it was found

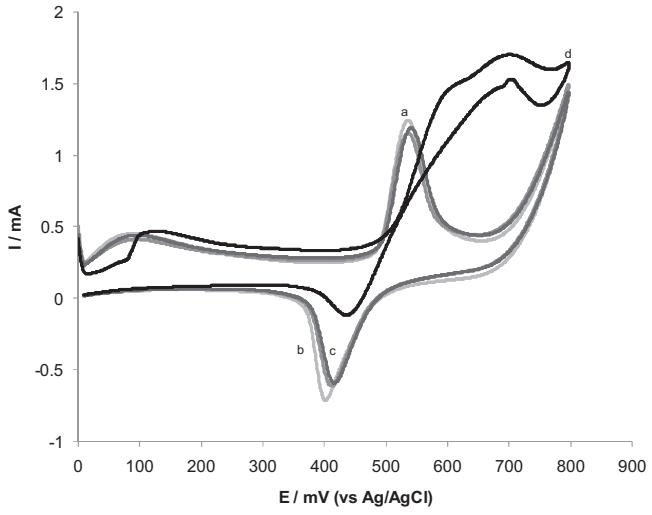

Fig. 5. Cyclic voltammograms corresponding to the addition of possible interfering species: (a) 2 mM of uric acid, (b) 0.2 mM of dopamine, (c) 0.3 mM of ascorbic acid, and (d) addition of 1.15 mM of glucose. The analytes were added sequentially to the same 0.1 M KOH solution.

that two factors are important, film thickness and the choice of an electrode material.

Yeo et al. have reported that a very thin layer of Ni hydroxide deposited onto Au has a significantly higher anodic oxygen evolution activity relative to a thick layer of Ni hydroxide formed on bulk Ni or electrodeposited on Au. Moreover, they have also reported that Au may modify the electronic properties of $Ni^{(III)}$ cations present in a thin film of NiOOH on its surface by a small transfer of charge to the highly electronegative Au [30].

In our case, the nickel surface concentration (Γ_{Ni}) was estimated in 4.9×10^{-9} mol cm^{-2} and corresponding to a thin layer of Ni oxide (<4 nm thick) [32].

Casella et al. have reported voltammetric and XPS studies of the catalytic behavior of the Au/Ni surface combination toward the electrooxidation of glucose with a thin nickel film. In this case, two redox transitions were observed in voltammograms: one is related to gold-oxide formation and re-formation of Au°, and the other is due to the $Ni^{(II)}/Ni^{(III)}$ system. It suggests that both active catalytic species such as Au(OH) ads and NiOOH lead to electrocatalytic oxidation of glucose [31,32]. This same behavior is observed when the electrode is modified in a solution without chloride ions (Fig. S1). Instead, Fig. 2 shows no redox transition related to oxidation/reduction of Au. Therefore, the formation of a thin film of nickel/nickel hydroxide in $EAuNi(OH)_2$ modified electrode is effective and the support material is completely covered.

In order to evaluate the properties of gold as substrate, a film of nickel was deposited on glassy carbon electrode ($GCNi(OH)_2$) following the same procedure. While a relation of $Ni^{(III)}/Ni^{(II)}$ of 0.63 is observed for $GCNi(OH)_2$ in the anodic peak, this ratio rose to 0.93 for $EAuNi(OH)_2$. This would suggest that Au could facilitate the oxidation of $Ni^{(II)}$ to $Ni^{(III)}$ and activate the nickel surface with suitable empty d-orbitals to rapidly catalyze the oxidation of the organic analyte [1].

The electrochemical performance of $EAuNi(OH)_2$ was studied by cyclic voltammetry in 0.1 M KOH solution at different scan rates. Both anodic and cathodic peak currents increase as function of scan rate. Fig. 3 shows a linear dependence for Ipa and Ipc with the square root of the scan rate, implying that the reaction is under diffusion control of OH^- from the solution phase.

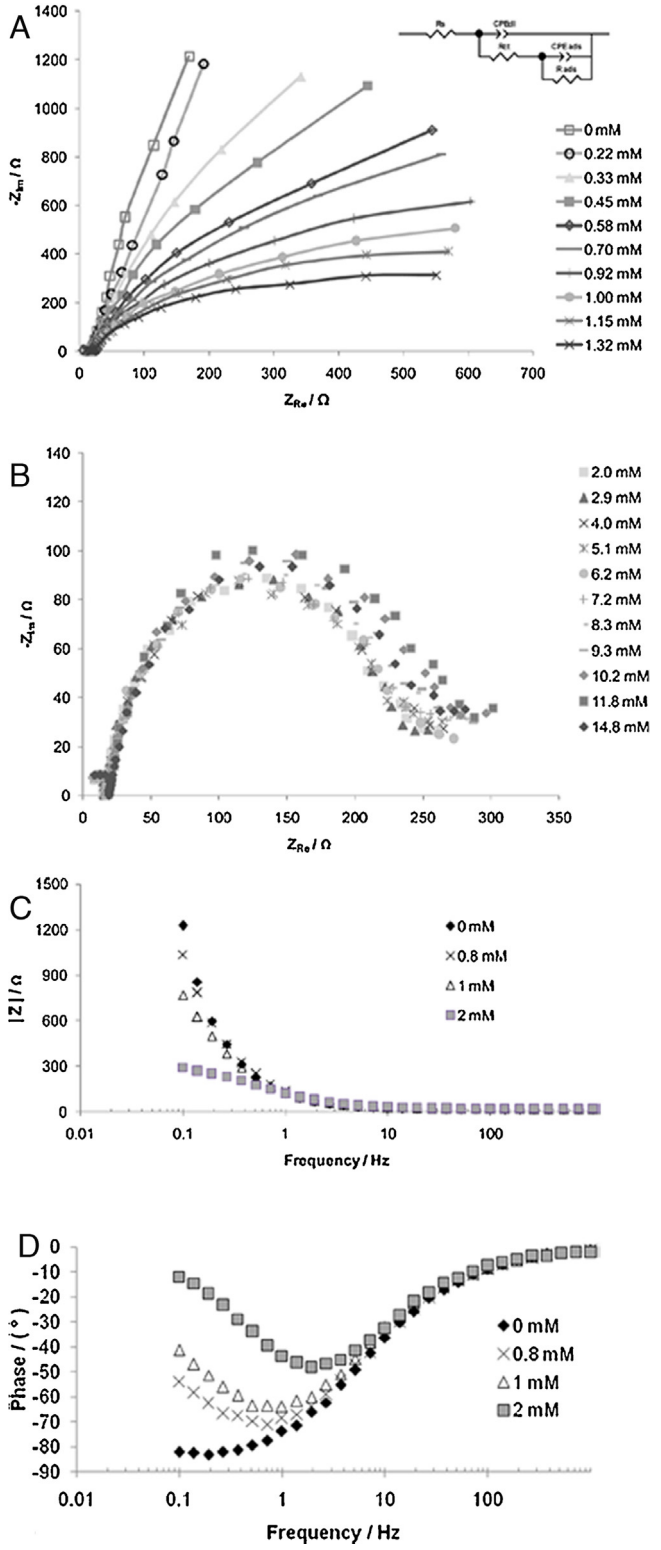

Fig. 6. (A) and (B) Nyquist plots for $EAuNi(OH)_2$ in 0.1 M KOH solution for 0–1.32 mM, and 2–14.8 mM glucose concentration ranges, respectively. Inset in Fig. 6(A) shows the equivalent circuit representation. (C) and (D) Bode plots for $EAuNi(OH)_2$ for the glucose concentration range of 0–2 mM.

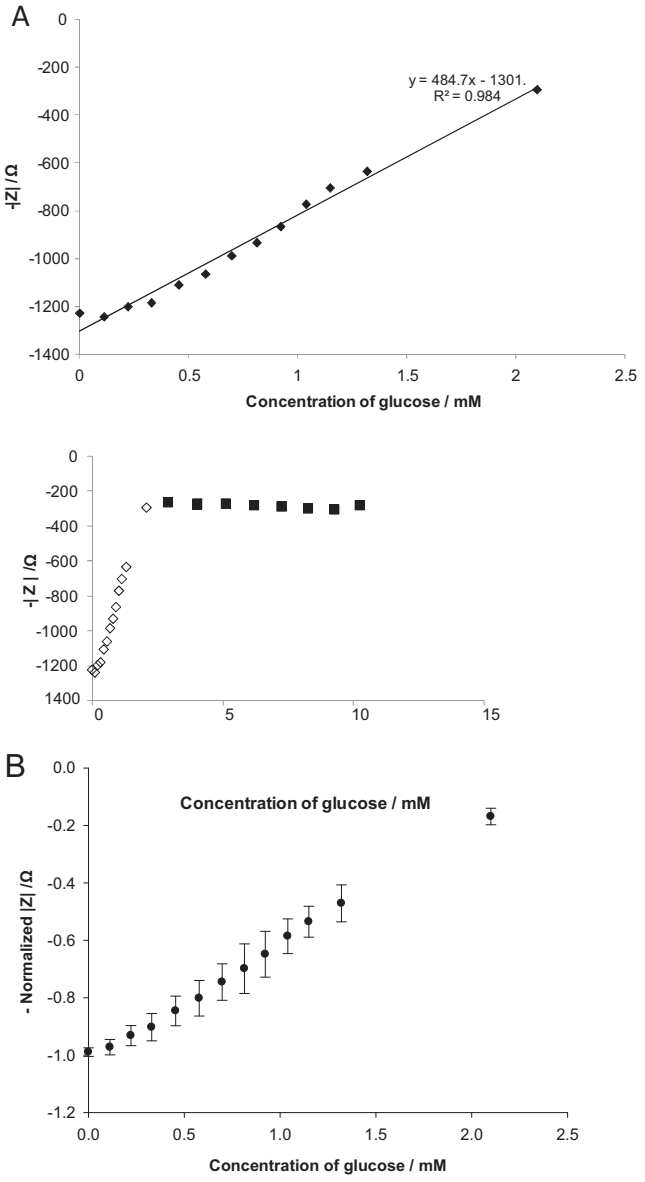

Fig. 7. (A) Module of impedance as a function of glucose concentration range of 0–16 mM. Inset shows module of impedance for the glucose concentration ranges of (◊) 0–2 mM and (■) 2.9–14.8 mM. (B) Normalized impedance magnitude against glucose concentration range of 0–2 mM. Both sets of data were obtained at 0.1 Hz and +0.500 V vs Ag/AgCl.

3.2. Electrocatalytic oxidation of glucose

The oxidation of glucose by EAuNi(OH)$_2$ was first studied by cyclic voltammetry in the range of 0–6.6 mM (Fig. 4A). The anodic peak current is linearly dependent to glucose concentration, increasing slightly in its presence (inset Fig. 4A). The response to glucose for EAuNi(OH)$_2$ was significantly bigger than that for EAu(OH)Ni(OH)$_2$ (Fig. S2). The anodic peak current is proportional to the square root of the scan rate (Fig. 4B) indicating a typical behavior for a mass transfer controlled reaction. In addition, the cathodic peak current corresponding to the reduction of $Ni^{(III)}$ to $Ni^{(II)}$ decreases, which is attributed to the production of Ni(OH)$_2$ through the reaction between NiOOH and glucose. A plot of $Ip/v^{1/2}$ with scan rate gives the same features as those revealed from Fig. 4C. This curve is characteristic of catalytic controlled reactions. In this way, EAuNi(OH)$_2$ shows a remarkable electrocatalytic activity toward the oxidation of glucose in 0.1 M KOH, as seen in the following reactions (Eq. (3)):

$$Ni(OH)_2 + OH^- \rightarrow NiOOH + H_2O + e^-$$

$$NiOOH + \text{glucose} \rightarrow Ni(OH)_2 + \text{intermediate}$$

$$NiOOH + \text{intermediate} \rightarrow Ni(OH)_2 + \text{gluconolactone}$$

Selectivity is a very important parameter to be considered for non-enzymatic glucose sensors. We studied the interference effect of uric acid (UA), dopamine (DA) and ascorbic acid (AA) in low (normal physiological levels [1]) and high concentrations. In low concentrations, no reaction was observed, whereas in higher concentrations, the response to interferents is seen at 0.1 V but that does not affect the oxidation of glucose. Fig. 5 shows the effect of 2 mM UA, 0.2 mM DA and 0.3 mM AA on the response of 1.15 mM glucose. When uric acid, dopamine and ascorbic acid were added successively in this order in 0.1 M KOH solution, one couple of well-defined $Ni^{(II)}/Ni^{(III)}$ redox peaks was observed without changes. Finally, a glucose concentration was added and the electrocatalytic response toward oxidation of glucose was obtained.

3.3. Electrochemical Impedance Spectroscopy (EIS) measurements

Electrochemical Impedance Spectroscopy (EIS) was used to evaluate the performance of EAuNi(OH)$_2$ as glucose sensor in a frequency range of 100 kHz–0.1 Hz. The amplitude of oscillation was set to 10 mV and the working potential was optimized to +0.500 V vs Ag/AgCl. Nyquist and Bode plots of the EAuNi(OH)$_2$ in 0.1 M KOH for different glucose concentrations are presented in Fig. 6.

In Fig. 6A, for a range of 0–2 mM of glucose, the Nyquist diagrams consist of two slightly depressed capacitive semicircles in the high and low frequencies. The depressed semicircle in high frequency region can be related to the combination of charge transfer resistance and the double layer capacitance. The low frequency semicircle was related to the adsorption of reaction intermediate on the electrode surface. The equivalent circuit compatible with the Nyquist diagram is depicted. In this electrical equivalent circuit, R_s, CPE_{dl} and R_{ct} represent solution resistance, a constant phase element corresponding to the double layer capacitance and the charge transfer resistance, respectively. CPE_{ads} and R_{ads} are the electrical elements related to the adsorption of reaction intermediates [44]. When glucose was added up to 2 mM to the cell, a decrease in the diameters of the two semicircles was observed (Fig. 6A), while for concentrations of glucose above 2 mM these did not change significantly under these experimental conditions (Fig. 6B).

Pletcher [5] suggested the electrocatalytic process implies a key role for adsorbed intermediates. In our case, we observed that in the concentration range up to 2 mM glucose the equivalent circuit model involves a component related to the adsorption of reaction intermediates. This would suggest that an initial oxidation of glucose limited to the surface would then give rise to bulk oxidation of glucose, as shown by the linear proportionality of peak current to square root of scan rate in Fig. 4B.

Although the method based in the evaluation of the R_{ct} as function of the glucose concentration could be employed for its quantification in a range of 0–2 mM of analyte, it is very laborious and extremely long, since R_{ct} must be obtained from an elemental electrical circuit fitted to a set of impedance values.

As an alternative, a single-frequency analysis can be proposed for EIS measurements of glucose. However, the optimal parameter of complex impedance (module, phase, real or imaginary impedance) and frequency values of the system must be previously determined.

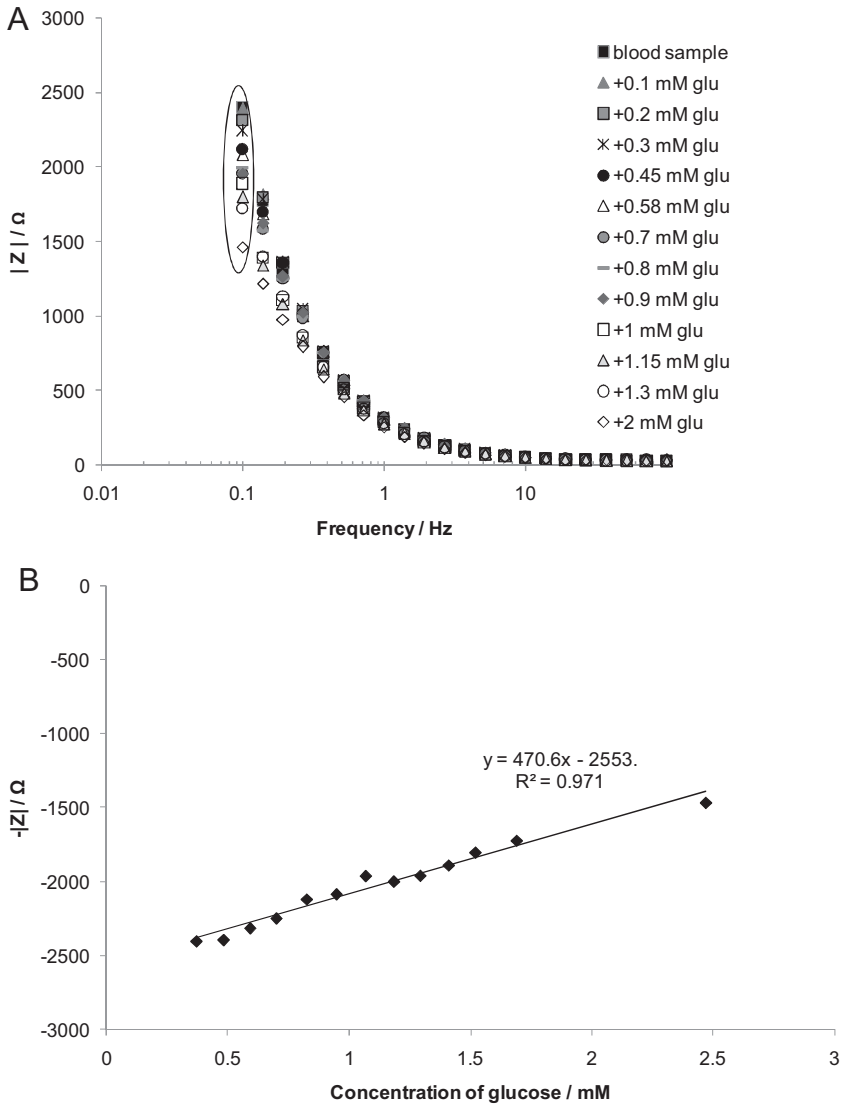

Fig. 8. (A) Bode plots for EAuNi(OH)2 of impedance module against frequency for the glucose concentration range of 0–2 mM in blood sample. (B) Calibration curve for module of impedance as a function of glucose concentration in blood at 0.1 Hz and +0.600 V vs Ag/AgCl.

In order to determine the optimal parameter and frequency for analytical measurement of glucose, the module (|Z|), phase (φ), real impedance (Zr), and imaginary impedance (Zi) of complex impedance were analyzed for each frequency and in function of glucose concentration, separately (Fig. S3). The correlation of each parameter with the glucose concentration for each frequency was studied in terms of correlation coefficient (R^2). These analyses show a better linear response for glucose concentration up to 2 mM, with a 0.984 correlation coefficient, for |Z| at 0.1 Hz. Fig. 7A shows the calibration curve for −|Z| as a function of the glucose concentration in a linear range from 0 to 2 mM, which is based on the average of eight values obtained in the time at 0.1 Hz for each glucose addition.

To be able to compare the repeatability of three modified electrodes it is necessary to evaluate the normalized impedance (relative value to zero concentration of glucose) (Fig. 7B). Triplicate sets of results show the repeatability and reproducibility corresponding to the measurements with a relative standard deviation (RSD) of less than 5% for a glucose concentration range of 0.1–0.5 mM and about 10% for high glucose concentration range (0.5–2 mM).

Table 1
Determination of glucose in blood samples using two different $EAuNi(OH)_2$ electrodes and impedance measurements. Comparison with values obtained by a commercial handheld glucose meter.

Blood sample	|Z| (ohms)[a]		Proposed method (mM)	Commercial handheld
	$EAuNi(OH)_2$ #1	$EAuNi(OH)_2$ #2		Glucose meter (mg dL^{-1})
1	2326.962	2309.759	5.0 ± 0.3 (100 mg dL^{-1})[b]	95
2	2151.718	2128.353	8.8 ± 0.4 (175 mg dL^{-1})[b]	172
3	1964.759	1932.917	12.8 ± 0.5 (257 mg dL^{-1})[b]	265

[a] The blood samples were diluted ten times with 0.1 M KOH solution for the impedance measurements.
[b] Glucose concentration expressed as mg dL^{-1}.

Table 2
Comparison of the present EAuNi(OH)$_2$ electrode with different non-enzymatic glucose sensors based on nickel.

Electrode	Catalyst	Potential (V)	Linear range (M)	Electrochemical method	Determination in blood sample	Ref.
Au-Ni electrode	$Au(OH)_{ads}$ and NiOOH	0.6 (vs Ag/AgCl)	6×10^{-8} to 7×10^{-4}	Amperometry	No	[31]
NiCFP[a]	NiO	0.6 (vs Ag/AgCl)	2×10^{-6} to 2.5×10^{-3}	Amperometry	No	[45]
NiNWA[b]	NiO/Ni(OH)$_2$	0.55 (vs SCE)	5×10^{-7} to 7×10^{-3}	Amperometry	No	[46]
Ni film Au nanoporous	$Au(OH)_{ads}$ and NiOOH	0.4 (vs SCE)	1×10^{-6} to 1×10^{-3}	Amperometry	No	[35]
Ni-AuBPE[c]	Ni(OH)$_2$	0.55 (vs Ag/AgCl)	up to 2×10^{-3}	Chronoamperometry	No	[47]
GC/MWCNT/NiO	NiO	0.6 (vs Ag/AgCl)	2×10^{-4} to 1.2×10^{-2}	Amperometry	Yes	[48]
Ni BDD	Ni(OH)$_2$	0.46 (vs SCE)	1×10^{-5} to 1×10^{-2}	Amperometry	No	[25]
NiO/NF[d]	NiO	0.47 (vs Ag/AgCl)	5×10^{-6} to 5.5×10^{-3}	Amperometry	Yes	[49]
EAuNi(OH)$_2$	NiOOH	0.6 (vs Ag/AgCl)	up to 2×10^{-3}	Single-frequency impedance	Yes	This work

[a] Carbon nanofiber paste.
[b] Nanowire arrays.
[c] Gold barrel plating electrode.
[d] Nickel foam.

3.4. Performance of EAuNi(OH)$_2$ in the determination of glucose in real samples

To further evaluate the applicability of EAuNi(OH)$_2$ in real samples, this modified electrode was used to determine glucose in human blood samples. As shown, the electrocatalytic oxidation of glucose requires an alkaline medium, thus the sample was diluted ten times with 0.1 M KOH solution. Fig. S4 shows the CVs for a blood sample with a glucose concentration of 0.45 mM (90 mg dL^{-1} measured by a commercial handheld glucose meter), and subsequent additions of glucose. It can be seen that EAuNi(OH)$_2$ shows a good catalytic activity for glucose even in the presence of the biological matrix and it is insensitive to electroactive interfering species commonly present in blood. The blood glucose levels should be able to be screened in the range of 40–400 mg dL^{-1} (2–20 mM). To determine glucose in the range of 0–2 mM due to dilution in 0.1 M KOH, impedance measurements were obtained for each sample as indicated in Section 2.5. The working potential was optimized to +0.600 V vs Ag/AgCl according to what was seen in CVs. The Nyquist plot for EAuNi(OH)$_2$ (Fig. S5) shows a decrease of R_{ct} values against increasing concentrations of glucose. Fig. 8A depicts |Z| in a frequency range of 0.1–100 Hz for each blood sample spiked with glucose standard. Finally, the single-frequency EIS measurements were obtained under optimal experimental conditions previously determined. The calibration curve for −|Z| as a function of the glucose concentration in blood at 0.1 Hz is shown in Fig. 8B. This demonstrates that the presence of blood can modify the absolute values of |Z| at 0.1 Hz in the glucose determination but does not change the slope significantly (470.6 vs 484.7 Ω mM^{-1} of glucose, with and without blood, respectively), and R^2 (0.971) is suitable. The lower limit of detection was 0.37 mM of glucose corresponding to a blood sample with the lowest blood sugar.

The single-frequency EIS measurements of |Z| at 0.1 Hz and +0.600 V vs Ag/AgCl for three blood samples using two different electrodes (EAuNi(OH)$_2$ #1 and EAuNi(OH)$_2$ #2) were obtained and the calibration curve (Fig. 8B) was applied. The results thus obtained together with those from a commercial handheld glucose meter are summarized in Table 1. As shown, there is a satisfactory agreement between the results obtained by the proposed impedance methodology using EAuNi(OH)$_2$ electrode and those measured by a commercial handheld glucose meter.

Table 2 summarizes some non-enzymatic glucose electrochemical sensors in which the experimental parameters directly compare to the procedure discussed in this paper. The gold surfaces modified with nickel are particularly included. From Table 2, it is evident that amperometry is the most popular electrochemical technique applied in glucose sensors.

4. Conclusions

A new approach on the modification of gold electrodes with a thin layer of Ni(OH)$_2$/NiOOH has been presented in this work. The highly electronegative Au seems to favor the generation of active catalytic species NiOOH, which is a strong oxidant. Moreover, the addition of high concentrations of chloride ions into the electrodeposition nickel solution avoids the presence of a mixed catalyst Au(OH) ads and NiOOH, which responds to oxidation of glucose in different ways. The repeated CVs of glucose by EAuNi(OH)$_2$ show no fouling due to adsorbed intermediates which might suggest a bulk oxidation of glucose catalyzed only by NiOOH.

Furthermore, we demonstrated that single-frequency impedance measurements can be applied to determine glucose with a non-enzymatic glucose electrode. EIS, as transduction method for EAuNi(OH)$_2$ electrode, displays the best relationship with the concentration of glucose for module of impedance (|Z|) at 0.1 Hz in the range of 0–2 mM of analyte in alkaline medium.

In this way, the unequivocal sensor response to glucose was determined not only by the catalyst on the electrode surface but also by the optimization of the impedance parameter, the frequency, and the working potential.

Finally, the correlation between impedance and concentration of glucose in a biological complex matrix was studied. The evaluation of interfering species normally found in whole blood and the good sensitivity for |Z| at 0.1 Hz and +0.600 V vs Ag/AgCl indicate that the EAuNi(OH)$_2$ electrode could be used for glucose detection in real samples in alkaline medium.

Acknowledgements

Financial support from the University of Buenos Aires (UBACyT 2014-17 20020130100469BA), ANPCyT (PICT 2012-0064 and PICT 2013-1541), and CONICET (11220130100029CO) are gratefully acknowledged. A.L. Rinaldi would like to thank CONICET for her doctoral fellowship.

Appendix A. Supplementary data

Supplementary data associated with this article can be found, in the online version, at http://dx.doi.org/10.1016/j.snb.2015.12.101.

References

[1] K.E. Toghill, R.G. Compton, Electrochemical non-enzymatic glucose sensors: a perspective and an evaluation, Int. J. Electrochem. Sci. 5 (2010) 1246–1301 http://www.electrochemsci.org/papers/vol5/5091246.pdf.

[2] Q. Wu, L. Wang, H. Yu, J. Wang, Z. Chen, Organization of glucose-responsive systems and their properties, Chem. Rev. 111 (2011) 7855–7875, http://dx.doi.org/10.1021/cr200027j.
[3] A. Heller, B. Feldman, Electrochemical glucose sensors and their applications in diabetes management, Chem. Rev. 108 (2008) 2482–2505, http://dx.doi.org/10.1021/cr068069y.
[4] S. Park, H. Boo, T.D. Chung, Electrochemical non-enzymatic glucose sensors, Anal. Chim. Acta 556 (2006) 46–57, http://dx.doi.org/10.1016/j.aca.2005.05.080.
[5] D. Pletcher, Electrocatalysis: present and future, J. Appl. Electrochem. 14 (1984) 403–415, http://dx.doi.org/10.1007/BF00610805.
[6] S.H. Kim, J.B. Choi, Q.N. Nguyen, J.M. Lee, S. Park, T.D. Chung, J.Y. Byun, Nanoporous platinum thin films synthesized by electrochemical dealloying for nonenzymatic glucose detection, Phys. Chem. Chem. Phys. 15 (2013) 5782–5787, http://dx.doi.org/10.1039/c2cp43097e.
[7] F. Kurniawan, V. Tsakova, V.M. Mirsky, Gold nanoparticles in nonenzymatic electrochemical detection of sugars, Electroanalysis 18 (2006) 1937–1942, http://dx.doi.org/10.1002/elan.200603607.
[8] Y. Ma, J. Di, X. Yan, M. Zhao, Z. Lu, Y. Tu, Direct electrodeposition of gold nanoparticles on indium tin oxide surface and its application, Biosens. Bioelectron. 24 (2009) 1480–1483, http://dx.doi.org/10.1016/j.bios.2008.10.007.
[9] F. Huang, Y. Zhong, J. Chen, S. Li, Y. Li, F. Wang, S. Feng, Nonenzymatic glucose sensor based on three different CuO nanomaterials, Anal. Methods 5 (2013) 3050–3055, http://dx.doi.org/10.1039/c3ay40342d.
[10] M. Jafarian, F. Forouzandeh, I. Danaee, F. Gobal, M.G. Mahjani, Electrocatalytic oxidation of glucose on Ni and NiCu alloy modified glassy carbon electrode, J. Solid State Electrochem. 13 (2009) 1171–1179, http://dx.doi.org/10.1007/s10008-008-0632-1.
[11] N.Q. Dung, D. Patil, H. Jung, D. Kim, A high-performance nonenzymatic glucose sensor made of CuO-SWCNT nanocomposites, Biosens. Bioelectron. 42 (2013) 280–286, http://dx.doi.org/10.1016/j.bios.2012.10.044.
[12] L. Luo, L. Zhu, Z. Wang, Nonenzymatic amperometric determination of glucose by CuO nanocubes-graphene nanocomposite modified electrode, Bioelectrochemistry 88 (2012) 156–163, http://dx.doi.org/10.1016/j.bioelechem.2012.03.006.
[13] M. Yousef Elahi, H. Heli, S.Z. Bathaie, M.F. Mousavi, Electrocatalytic oxidation of glucose at a Ni-curcumin modified glassy carbon electrode, J. Solid State Electrochem. 11 (2007) 273–282, http://dx.doi.org/10.1007/s10008-006-0104-4.
[14] N. Hui, S. Wang, H. Xie, S. Xu, S. Niu, X. Luo, Nickel nanoparticles modified conducting polymer composite of reduced graphene oxide doped poly(3,4-ethylenedioxythiophene) for enhanced nonenzymatic glucose sensing, Sens. Actuators B: Chem. 221 (2015) 606–613, http://dx.doi.org/10.1016/j.snb.2015.07.011.
[15] F. Cao, S. Guo, H. Ma, G. Yang, S. Yang, J. Gong, Highly sensitive nonenzymatic glucose sensor based on electrospun copper oxide-doped nickel oxide composite microfibers, Talanta 86 (2011) 214–220, http://dx.doi.org/10.1016/j.talanta.2011.09.003.
[16] X. Zhang, Q. Liao, S. Liu, W. Xu, Y. Liu, Y. Zhang, CuNiO nanoparticles assembled on graphene as an effective platform for enzyme-free glucose sensing, Anal. Chim. Acta 858 (2015) 49–54, http://dx.doi.org/10.1016/j.aca.2014.12.007.
[17] X. Zhang, A. Gu, G. Wang, Y. Wei, W. Wang, H. Wu, B. Fang, Fabrication of CuO nanowalls on Cu substrate for a high performance enzyme-free glucose sensor, CrystEngComm 12 (2010) 1120–1126, http://dx.doi.org/10.1039/b919749d.
[18] A.J. Wang, J.J. Feng, Z.H. Li, Q.C. Liao, Z.Z. Wang, J.R. Chen, Solvothermal synthesis of Cu/Cu_2O hollow microspheres for non-enzymatic amperometric glucose sensing, CrystEngComm 14 (2012) 1289–1295, http://dx.doi.org/10.1039/C1CE05869J.
[19] Q. Yang, M. Long, L. Tan, Y. Zhang, J. Ouyang, P. Liu, A. Tang, Helical TiO_2 nanotube arrays modified by Cu–Cu_2O with ultrahigh sensitivity for the nonenzymatic electro-oxidation of glucose, ACS Appl. Mater. Interfaces 7 (2015) 12719–12730, http://dx.doi.org/10.1021/acsami.5b03401.
[20] S. Yu, X. Peng, G. Cao, M. Zhou, L. Qiao, J. Yao, H. He, Ni nanoparticles decorated titania nanotube arrays as efficient nonenzymatic glucose sensor, Electrochim. Acta 76 (2012) 512–517, http://dx.doi.org/10.1016/j.electacta.2012.05.079.
[21] M. Fleischmann, K. Korinek, D. Pletcher, The oxidation of organic compounds at a nickel anode in alkaline solution, J. Electroanal. Chem. Interfacial Electrochem. 31 (1971) 39–49, http://dx.doi.org/10.1016/s0022-0728(71)80040-2.
[22] H. Liu, F. Favier, K. Ng, M.P. Zach, R.M. Penner, Size-selective electrodeposition of meso-scale metal particles: a general method, Electrochim. Acta 47 (2001) 671–677, http://dx.doi.org/10.1016/s0013-4686(01)00747-2.
[23] D.S. Hall, D.J. Lockwood, C. Bock, B.R. MacDougall, Nickel hydroxides and related materials: a review of their structures, synthesis and properties, Proc. R. Soc. A 471 (2015), http://dx.doi.org/10.1098/rspa.2014.0792, 20140792.
[24] L.A. Hutton, M. Vidotti, A.N. Patel, M.E. Newton, P.R. Unwin, J.V. Macpherson, Electrodeposition of nickel hydroxide nanoparticles on boron-doped diamond electrodes for oxidative electrocatalysis, J. Phys. Chem. C 115 (2010) 1649–1658, http://dx.doi.org/10.1021/jp109526b.
[25] K.E. Toghill, L. Xiao, M.A. Phillips, R.G. Compton, The non-enzymatic determination of glucose using an electrolytically fabricated nickel microparticle modified boron-doped diamond electrode or nickel foil electrode, Sens. Actuators B: Chem. 147 (2010) 642–652, http://dx.doi.org/10.1016/j.snb.2010.03.091.
[26] M. Vidotti, C.D. Cerri, R.F. Carvalhal, J.C. Dias, R.K. Mendes, S.I. Cordoba de Torresi, L.T. Kubota, Nickel hydroxide electrodes as amperometric detectors for carbohydrates in flow injection analysis and liquid chromatography, J. Electroanal. Chem. 636 (2009) 18–23, http://dx.doi.org/10.1016/j.jelechem.2009.09.006.
[27] A.M. Ghonim, B.E. El-Anadouli, M.M. Saleh, Electrocatalytic glucose oxidation on electrochemically oxidized glassy carbon modified with nickel oxide nanoparticles, Electrochim. Acta 114 (2013) 713–719, http://dx.doi.org/10.1016/j.electacta.2013.10.115.
[28] H. Liu, X. Wu, B. Yang, Z. Li, L. Lei, X. Zhang, Three-dimensional porous NiO nanosheets vertically grown on graphite disks for enhanced performance non-enzymatic glucose sensor, Electrochim. Acta 174 (2015) 745–752, http://dx.doi.org/10.1016/j.electacta.2015.06.062.
[29] M.A. Kiani, M. Abbasnia Tehrani, H. Sayahi, Reusable and robust high sensitive non-enzymatic glucose sensor based on $Ni(OH)_2$ nanoparticles, Anal. Chim. Acta 839 (2014) 26–33, http://dx.doi.org/10.1016/j.aca.2014.06.016.
[30] B.S. Yeo, A.T. Bell, In situ raman study of nickel oxide and gold-supported nickel oxide catalysts for the electrochemical evolution of oxygen, J. Phys. Chem. C 116 (2012) 8394–8400, http://dx.doi.org/10.1021/jp3007415.
[31] I.G. Casella, M.R. Guascito, T.R.I. Cataldi, Electrocatalysis and amperometric detection of alditols and sugars at a gold-nickel composite electrode in anion-exchange chromatography, Anal. Chim. Acta 398 (1999) 153–160, http://dx.doi.org/10.1016/s0003-2670(99)00420-1.
[32] I.G. Casella, M.R. Guascito, M.G. Sannazzaro, Voltammetric and XPS investigations of nickel hydroxide electrochemically dispersed on gold surface electrodes, J. Electroanal. Chem. 462 (1999) 202–210, http://dx.doi.org/10.1016/s0022-0728(98)00413-6.
[33] I.G. Casella, M. Gatta, Electrochemical and XPS characterization of composite modified electrodes obtained by nickel deposition on noble metals, Anal. Chem. 72 (2000) 2969–2975, http://dx.doi.org/10.1021/ac9913863.
[34] S. Berchmans, V. Yegnaraman, N. Sandhyarani, K.V.G.K. Murty, T. Pradeep, Formation of a nickel hydroxide monolayer on Au through a self-assembled monolayer of 5,5-dithiobis(2-nitrobenzoic acid): voltammetric, SERS and XPS investigations of the modified electrodes, J. Electroanal. Chem. 468 (1999) 170–179, http://dx.doi.org/10.1016/s0022-0728(99)00163-1.
[35] J.-F. Huang, Facile preparation of an ultrathin nickel film coated nanoporous gold electrode with the unique catalytic activity to oxidation of glucose, Chem. Commun. (2009) 1270–1272, http://dx.doi.org/10.1039/b819658c.
[36] R.K. Shervedani, A.H. Mehrjardi, N. Zamiri, A novel method for glucose determination based on electrochemical impedance spectroscopy using glucose oxidase self-assembled biosensor, Bioelectrochemistry 69 (2006) 201–208, http://dx.doi.org/10.1016/j.bioelechem.2006.01.003.
[37] H. Wang, H. Ohnuki, H. Endo, M. Izumi, Impedimetric and amperometric bifunctional glucose biosensor based on hybrid organic-inorganic thin films, Bioelectrochemistry 101 (2015) 1–7, http://dx.doi.org/10.1016/j.bioelechem.2014.06.007.
[38] C.C. Mayorga Martinez, E.F. Treo, R.E. Madrid, C.C. Felice, Real-time measurement of glucose using chrono-impedance technique on a second generation biosensor, Biosens. Bioelectron. 29 (2011) 200–203, http://dx.doi.org/10.1016/j.bios.2011.08.018.
[39] C.C. Mayorga-Martinez, M. Gui, R.E. Madrid, A. Merkoi, Bimetallic nanowires as electrocatalysts for nonenzymatic real-time impedancimetric detection of glucose, Chem. Commun. 48 (2012) 1686–1688, http://dx.doi.org/10.1039/c2cc16601a.
[40] J.C. Hoogvliet, M. Dijksma, B. Kamp, W.P. van Bennekom, Electrochemical pretreatment of polycrystalline gold electrodes to produce a reproducible surface roughness for self-assembly: a study in phosphate buffer pH 7.4, Anal. Chem. 72 (2000) 2016–2021, http://dx.doi.org/10.1021/ac991215y.
[41] C.C. Streinz, A.P. Hartman, S. Motupally, J.W. Weidner, The effect of current and nickel nitrate concentration on the deposition of nickel hydroxide films, J. Electrochem. Soc. 142 (*1995*) 1084–1089, http://dx.doi.org/10.1149/1.2044134.
[42] F. Nasirpouri, S.M. Janjan, S.M. Peighambari, M.G. Hosseini, A. Akbari, A.S. Samardak, Refinement of electrodeposition mechanism for fabrication of thin nickel films on *n*-type silicon (1 1 1), J. Electroanal. Chem. 690 (2013) 136–143, http://dx.doi.org/10.1016/j.jelechem.2012.07.005.
[43] R. Oriňáková, M. Strečková, L. Trnková, R. Rozik, M. Gálová, Comparison of chloride and sulphate electrolytes in nickel electrodeposition on a paraffin impregnated graphite electrode, J. Electroanal. Chem. 594 (2006) 152–159, http://dx.doi.org/10.1016/j.jelechem.2006.05.031.
[44] I. Danaee, M. Jafarian, F. Forouzandeh, F. Gobal, M.G. Mahjani, Impedance spectroscopy analysis of glucose electro-oxidation on Ni-modified glassy carbon electrode, Electrochim. Acta 53 (2008) 6602–6609, http://dx.doi.org/10.1016/j.electacta.2008.04.042.
[45] Y. Liu, H. Teng, H. Hou, T. You, Nonenzymatic glucose sensor based on renewable electrospun Ni nanoparticle-loaded carbon nanofiber paste electrode, Biosens. Bioelectron. 24 (2009) 3329–3334, http://dx.doi.org/10.1016/j.bios.2009.04.032.
[46] L.-M. Lu, L. Zhang, F. Qu, H. Lu, X. Zhang, Z. Wu, S. Huan, Q. Wang, G. Shen, R. Yu, A nano-Ni based ultrasensitive nonenzymatic electrochemical sensor for glucose: enhancing sensitivity through a nanowire array strategy, Biosens. Bioelectron. 25 (2009) 218–223, http://dx.doi.org/10.1016/j.bios.2009.06.041.
[47] C.-Y. Tai, J.-L. Chang, J.-M. Zen, Easy preparation of a reticular nickel film deposited on a barrel-plating gold electrode with a high catalytic activity

towards the oxidation of glucose, Chem. Commun. 40 (2009) 6083–6085, http://dx.doi.org/10.1039/b912442j.
[48] M. Shamsipur, M. Najafi, M.-R. Milani Hosseini, Highly improved electrooxidation of glucose at a nickel(II) oxide/multi-walled carbon nanotube modified glassy carbon electrode, Bioelectrochemistry 77 (2010) 120–124, http://dx.doi.org/10.1016/j.bioelechem.2009.07.007.
[49] C. Guo, Y. Wang, Y. Zhao, C. Xu, Non-enzymatic glucose sensor based on three dimensional nickel oxide for enhanced sensitivity, Anal. Methods 5 (2013) 1644–1647, http://dx.doi.org/10.1039/C3AY00067B.

Biographies

A. Rinaldi received her B. Sc. in Biochemistry from the University of Buenos Aires in 2013. She is currently a graduate student at the Department of Analytical Chemistry and Physical Chemistry in the School of Pharmacy at the University of Buenos Aires, with Dr R. R. Carballo as supervisor. Her research area is the design of phases with molecular recognition ability for sensors applications of bioanalytes.

R.R. Carballo obtained her Ph.D. in Analytical Chemistry in 2007 from the University of Buenos Aires. She performed postdoctoral research in the group of Molecular Electrochemistry at the INQUIMAE Lab, School of Exact and Natural Sciences (University of Buenos Aires). At present, she is Adjunct Researcher at CONICET at the Department of Analytical Chemistry and Physical Chemistry in the School of Pharmacy at the University of Buenos Aires. Her research area is the development of electrochemical and optical sensors and biosensors.